TASK QUARTERLY 7 No 3 (2003), 409–424

DROP BREAK-UP AND COALESCENCE IN A STIRRED TANK

WIOLETTA PODGÓRSKA AND JERZY BAŁDYGA

Department of Chemical and Process Engineering,
Warsaw University of Technology,
Waryńskiego 1, 00-645 Warsaw, Poland
{*podgorsw,baldyga*}*@ichip.pw.edu.pl*

(Received 2 December 2002)

Abstract: It is shown in the paper that drop size distribution in liquid-liquid dispersions is affected by both the fine-scale and the large-scale inhomogeneity of turbulence. Fine-scale inhomogeneity is related to the phenomenon of local intermittency and described using a multifractal formalism. Large-scale inhomogeneity is related to inhomogeneous distributions of the locally averaged properties of turbulence, including the rate of energy dissipation and the integral scale of turbulence. Large-scale distributions of the properties of turbulence in a stirred tank are considered with a network of well-mixed zones. CFD methods are used to compute the properties of turbulence in these zones. A model taking into account inhomogeneity of both types explains the effect of the system's scale on drop size; it predicts smaller maximum stable drop sizes than the classic Kolmogorov theory of turbulence. The model predictions agree well with experimental data.

Keywords: CFD, intermittence, large-scale inhomogeneity, small-scale inhomogeneity

Notation

Symbols
a – film radius [m],
A – the Hamaker constant [J],
C_1', C_2' – the constants of the She and Leveque model of turbulence,
C_g, C_x – the constants of the breakage model,
C_p – the proportionality constant of order unity,
$d_{\max}$ – maximum stable drop diameter [m],
$d_{\max}^0$ – maximum stable drop diameter when neglecting intermittency [m],
d – drop diameter [m],
d_s – space dimension,
D_q – generalized dimension,
D – impeller diameter [m],
E_L, E_r – total energy dissipated in boxes of size L, and r [J],
$f_d(\alpha)$ – multi-fractal spectrum,
$f(\alpha)$ – multi-fractal spectrum $f_d(\alpha)$ for $d_s = 1$,
$f(d_j,d_k)$ – drop collision frequency [$\mathrm{m^{-3}s^{-1}}$],
F – interaction force [N],
$g(d,\vec{x},t)$ – break-up rate of drops of diameter d at position $\vec{x}$ at time t [$\mathrm{s^{-1}}$],

$g(v,\vec{x},t)$ – break-up rate of drops of volume v at position $\vec{x}$ at time t [s^{-1}],
h_f – film thickness [m],
h_c – critical film thickness [m],
h_0 – initial film thickness [m],
$h(v,v',\vec{x},t)$ – drop collision function [m^3s^{-1}],
L – integral scale of turbulence [m],
$n(v,\vec{x},t)$ – number density of drops of volume v at position $\vec{x}$ at time t [m^{-6}],
N – impeller rotational speed [s^{-1}],
p – pressure [Pa],
$\underline{p(d,\alpha)}$ – pressure stress acting upon a drop of diameter d [Pa],
$\overline{p(d)}$ – pressure stress acting upon a drop of diameter d according to the Kolmogorov theory [Pa],
$P(\alpha)$ – the probability density function for α,
r – distance [m],
R – drop diameter [m],
t_c – coalescence time [s],
$\bar{t}$ – contact time [s],
t – time [s],
T – tank diameter [m],
u, u_i – velocity, velocity component [ms^{-1}],
u_L – the rms velocity fluctuation [ms^{-1}],
u_r – velocity difference over distance r [ms^{-1}],
v, v' – drop volume [m^3],
We – the Weber number for a stirred tank ($=N^2D^3\rho_C/\sigma$),
$\vec{x}$ – position vector.

Greek Letters
$\alpha_{\min}$ – infimum of multifractal exponent α,
α – the multifractal exponent,
$\beta(v,v')$ – the probability density function for daughter drops [m^{-3}],
ε – turbulent energy dissipation rate per unit mass [m^2s^{-3}],
$\langle\varepsilon\rangle$ – ensemble average of ε [m^2s^{-3}],
$\langle\eta\rangle$ – the Kolmogorov microscale [m],
$\lambda(v,v')$ – coalescence efficiency,
λ – the scaling factor,
μ – dynamic viscosity [$kgm^{-1}s^{-1}$],
$\nu(v)$ – number of drops formed per breakage of drop of volume v,
ρ – density [kgm^{-3}],
$\rho(\alpha)$ – the pre-factor of Equation (4),
σ – interfacial tension [Nm^{-1}],
ϕ_j – average energy dissipation rate in a j-zone normalized with the average in the tank,
ϕ – dispersed phase volume fraction,
ζ – smaller to larger colliding drops radii ratio.

Subscripts
C – continuous phase,
D – dispersed phase.

1. Introduction

Liquid-liquid dispersions play an important role in many industrial processes, including heterogeneous chemical reactions, extraction, emulsion and suspension polymerization, and emulsion preparation. Stirred tanks are the most popular equipment to carry out these operations. The geometry and scale of the vessel and impeller,

the agitation rate and physical properties of the mixed phases determine the drop breakage and coalescence rates and the resulting drop size distributions.

Prediction of drop size distributions and the dynamics of their evolution is thus important from a practical point of view. The phenomenon of drop dispersion has been studied by many researchers, starting with the fundamental works by Kolmogorov [1] and Hinze [2]. Using the theory of fine-scale turbulence (Kolmogorov [3]) they have found that the maximum stable drop size, $d^0_{\max}$, could be related to the local rate of energy dissipation $\langle\varepsilon\rangle$ by:

$$d^0_{\max} = C_x \sigma^{0.6} \langle\varepsilon\rangle^{-0.4} \rho_C^{-0.6} = DWe^{-0.6}. \tag{1}$$

To describe the evolution of drop size distribution based on the Kolmogorov theory, breakage and coalescence functions (see for example [4–6]) were derived and used together with the relevant population balance equations. Large scale inhomogeneities of turbulence were either neglected or simulated by dividing the stirred tank into 2 or more (up to 11) subregions differing in turbulence properties [7].

Many experimental data agree quite well with the above mentioned models based on Kolmogorov's theory of turbulence. However, other experimental data could not be explained in this approach. This includes the variation of drop size distribution at long agitation times [8–10], time variation of the exponent on the Weber number [11, 12], scale-up effects [8, 13, 14] and the influence of impeller type on drop size [14, 15]. In this paper, the effects of fine-scale and large-scale inhomogeneity of turbulence on drop size distributions in stirred tanks are discussed.

2. Intermittent character of turbulence

Bałdyga and Bourne [12] suggested that a gradual decrease of the exponent on the Weber number with agitation time and the effect of scale of the system on the maximum stable drop size result from the phenomenon of fine-scale intermittency. As the result of intermittency, the rate of turbulent energy dissipation, turbulent vorticity and turbulent stresses are not distributed in a uniform manner. They show instead a large variability of their local and instantaneous values in time and space. Even in a statistically homogeneous turbulence there are events of both violent and quiet turbulence. Distributions of the energy dissipation rate, ε, in a turbulent field presented by Meneveau and Sreenivasan [16] display a spiky character. Intermittent distribution of the energy dissipation rate is schematically presented in Figure 1.

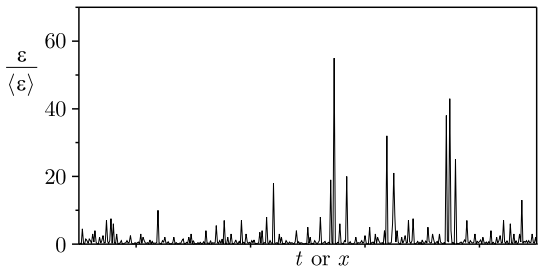

Figure 1. Intermittent character of turbulence

These strong non-uniformities increase with an increase of the Reylolds number. Intermittent character of turbulence at small scales has been known since the

experimental studies of Batchelor and Towsend [17]. There is no self-similarity of the turbulent velocity field at inertial subrange scales and the velocity structure functions do not satisfy the Kolmogorov [3] prediction that $\langle u_r^p \rangle = (\langle \varepsilon \rangle r)^{p/3}$. The fine-scale intermittency can be practically characterized by the exponent of the structure function ξ_p, $\langle u_r^p \rangle \sim r^{\xi_p}$. The discrepancy between the measured exponent ξ_p and $p/3$ increases with increasing p. The Kolmogorov theory agrees with experimental data for $p \approx 1$.

In the case of drop break-up, the normal pressure stresses acting upon drops are given by:

$$p(d) = C_p \rho_c [u_r(d)]^2, \tag{2}$$

so the second order velocity structure function influences the process.

In the classic theory of turbulence, it is assumed that energy is transported from large-energy eddies of scale L to the successive generations, n, of eddies of scales $r = (1/2)^n L$, and finally dissipated in the smallest eddies of size $\langle \eta \rangle$. The small eddies occupy the same space as the large ones, so the number of eddies per unit volume grows with the number of generation as $(1/2)^{-3n}$. The simplest way to take intermittency into account is to assume that there is a fraction of hydrodynamically active fluid and the rest of the fluid is hydrodynamically inactive. The energy dissipation rate, ε, thus either assumes a constant value greater than the mean value or equals zero. The number of daughter eddies is chosen so that the fraction of volume occupied by active eddies decreases by a factor from the range (0,1) to give a fraction of active space $\beta(r) = (r/L)^{3-D_\beta}$. This model, called the β-model, was introduced by Frisch, Sulem and Nelkin [18]. D_β is interpreted as a fractal dimension.

A more elaborated model of the fine structure of turbulence was proposed by Frisch and Parisi [19]. They introduced a multifractal model starting from the Navier-Stokes equations that are invariant after the following set of rescaling transformations: $x_i' = \lambda x_i$, $u_i' = \lambda^{\alpha/3} t$, $t' = \lambda^{1-\alpha/3} t$, provided that $\langle \eta \rangle < r, r' < L$ and $L >>> \langle \eta \rangle$, where $r = \sqrt{(x_i^2)}$. Local pressure, which is highly intermittent, transforms as u_i^2 or scales as $p' = \lambda^{2\alpha/3} p$. This enables us to show how the velocity increment over a distance r, u_r, behaves under the above transformations:

$$u_r = [\langle \varepsilon \rangle r]^{1/3} (r/L)^{\frac{\alpha-1}{3}}. \tag{3}$$

The turbulent events labelled by the scaling exponent α appear in a d_s-dimensional space with probability $P(\alpha)d\alpha$, where the probability density function is defined as (Chhabra *et al.* [20]):

$$P(\alpha) \cong \rho(\alpha) \sqrt{\ln(L/r)} (r/L)^{d_s - f_d(\alpha)}. \tag{4}$$

Sensitivity $\rho(\alpha)$ to α is small and can be neglected. $f_d(\alpha)$ is a multifractal spectrum and can be interpreted as a fractal dimension. As α characterizes the strength of singularities, the curve $f_d(\alpha)$ may also be regarded as a singularity spectrum. The multifractal spectrum $f_d(\alpha)$ can be related to the distribution of a generalized dimension D_q by using the Legendre transformation. Relation between D_q and q:

$$\sum E_r^q \sim E_L^q (r/L)^{D_q(q-1)}, \tag{5}$$

where E_r and E_L are total energy dissipations in boxes of size r and L, respectively, in a d_s-dimensional space, was measured by Meneveau and Sreenivasan [16] and

recalculated into a multifractal spectrum $f_d(\alpha)$. The $f_d(\alpha)$ function has a single maximum and can be well approximated around the maximum by a second order expansion, [21]. The parabolic distribution of $f_d(\alpha)$ is equivalent to log-normal distribution of the energy dissipation rate [22, 23] and agrees with experimental results for $0.51 < \alpha < 1.78$. Unfortunately, the most violent bursts of turbulence are characterized by small values of α ($\alpha < 0.5$), where the difference between the parabolic approximation of $f_d(\alpha)$ and the experimental data increases. The minimum α-value, $\alpha_{\min} = 0.12$, characterizing rare, but most vigorous, turbulent events was extrapolated using square-root-exponential probability distribution (Meneveau and Sreenivasan [16]). For practical reasons, Bałdyga and Podgórska [24] have fitted the function $f(\alpha)(d_s = 1)$ for the experimental data of Meneveau and Sreenivasan [16]:

$$f(\alpha) = a + b\alpha + c\alpha^2 + d\alpha^3 + e\alpha^4 + f\alpha^5 + g\alpha^6 + h\alpha^7 + i\alpha^8, \tag{6}$$

where $a = -3.51$, $b = 18.721$, $c = -55.918$, $d = 120.90$, $e = -162.54$, $f = 131.51$, $g = -62.572$, $h = 16.10$, $i = -1.7264$. Another form of the multifractal spectrum function $f_d(\alpha)$ was proposed by She and Leveque [25]:

$$f_d(\alpha) = 1 + C_1'(\alpha - 1/3) - C_2'(\alpha - 1/3)\ln[(\alpha - 1/3)/3], \tag{7}$$

where $C_1' = [(1 + \ln(\ln 3/2))/\ln 3/2 - 1]$, $C_2' = (\ln(3/2))^{-1}$. In this model the minimum value of the multifractal exponent α is larger than the value approximated by Meneveau and Sreenivasan [16] and equals $\alpha_{\min} = 1/3$.

2.1. The influence of fine-scale inhomogeneity on drop breakage and drop coalescence

Using Equations (2) and (3), Bałdyga and Bourne [12, 26] derived the relation for normal stresses acting upon a particle whose diameter, d, falls whithin the inertial subrange of intermittent turbulence:

$$p(d,\alpha) = C_p\rho[\langle\varepsilon\rangle d]^{2/3}(d/L)^{\frac{2}{3}\alpha - 1} = \overline{p(d)}(d/L)^{\frac{2}{3}\alpha - 1}. \tag{8}$$

The most violent events creating the largest turbulent stresses are labelled by $\alpha_{\min}$. The probability of such events is very small and their influence on the process can be observed after long periods of time. The most probable stresses labelled by α-values close to 1 are much smaller (see Figure 2).

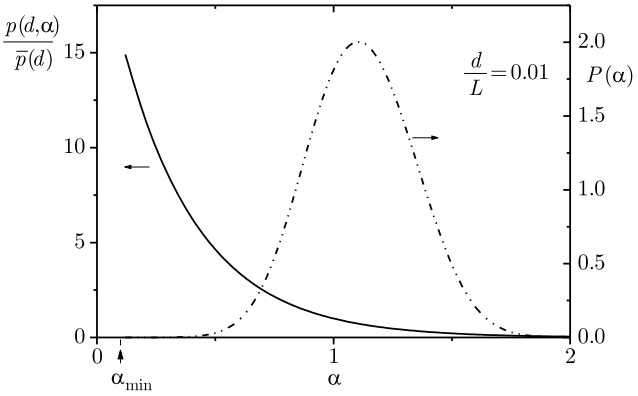

Figure 2. Distribution of normalized normal pressure stresses and the probability density function of stresses labelled by multifractal exponent α

The maximum stable drop size in diluted non-coalescing dispersion can be predicted by comparing dispersive turbulent stresses and stabilizing stresses due to the interfacial tension, σ, for the case of low viscosity of the dispersed phase (Bałdyga and Podgórska [24]):

$$d_{\max} = C_x^{\frac{5}{3+2\alpha}} L(\sigma\rho_c^{-1}\langle\varepsilon\rangle^{-2/3}L^{-5/3})^{\frac{3}{3+2\alpha}}. \tag{9}$$

For a stirred tank, the integral scale L is proportional to the diameter of the stirrer, D, and one gets:

$$d_{\max}/D = C_1(\alpha)\mathrm{We}^{\frac{-0.6}{1-0.4(1-\alpha)}}. \tag{10}$$

The most probable result is close to the solution when intermittency is neglected. In such case, $\alpha = 1$ and the exponent on the Weber number in Equation (10) is -0.6, as in Equation (1). For $\alpha < 1$, the stresses acting on drops are higher, hence the quasi-stable drop size is described by $\alpha_{\min} < \alpha < 1$, and an asymptotically stable drop is characterized by $\alpha_{\min}$. For $\alpha_{\min} = 0.12$, the exponent on the Weber number is equal to -0.926, which is close to the -0.93 exponent observed in experiments by Konno and Saito [11]. If the value of $\alpha_{\min}$ given by She and Leveque [25] is assumed, then the exponent on the Weber number is equal to -0.818. It means that asymptotically stable drops larger than for $\alpha_{\min} = 0.12$ are predicted. The break-up rate of drops of diameter d, $g(d)$, was derived by Bałdyga and Podgórska [24] by summing up the contributions to the break-up frequency from all the sufficiently vigorous eddies:

$$g(d) = C_g\sqrt{\ln(L/d)}\ \langle\varepsilon\rangle^{1/3}\ d^{-2/3}\int_{\alpha_{\min}}^{\alpha_x}(d/L)^{\frac{\alpha+2-3f(\alpha)}{3}}d\alpha, \tag{11}$$

with the upper limit of integral $\alpha_x = 2.5\ln(L\langle\varepsilon\rangle^{0.4}\rho_c^{0.6}\sigma^{-0.6}C_x^{-1})/\ln(L/d) - 1.5$, and $f(\alpha)$ given by Equation (6). The multifractal model of turbulence enables us to predict the influence of the system scale on the drop break-up rate (see Figure 3). It can be seen that in larger systems (larger integral scale of turbulence L) the drop break-up rate is higher.

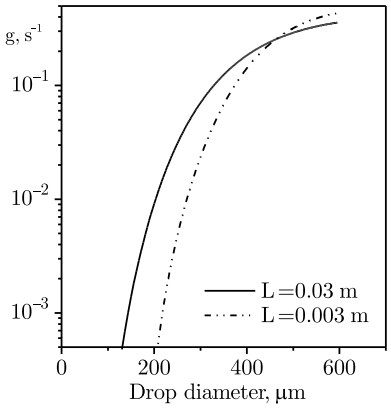

Figure 3. The influence of the system scale on the drop break-up rate

A multifractal approach was also used to model the coalescence process. The local average value of the coalescence rate is given by a product of drop collision

frequency, $f(d_j,d_k)$, and coalescence efficiency, $\lambda(d_j,d_k)$. The collision frequency is governed by the external flow of the continuous phase. Assuming orthokinetic drop collisions, Podgórska and Bałdyga [27, 28] derived the following expression for the case of intermittent turbulence:

$$f(d_j,d_k)=h(d_j,d_k)n_jn_k=C_{in}\langle\varepsilon\rangle^{1/3}\left(\frac{d_j+d_k}{2}\right)^{7/3}\left(\frac{d_j+d_k}{2L}\right)^{0.027}n_jn_k. \tag{12}$$

This equation shows that intermittency decreases slightly the collision rate relative to the case of a uniform energy dissipation rate. This effect can be observed in large scale systems, where $(d_j+d_k)/L<<1$. The coalescence efficiency, $\lambda(d_j,d_k)$, depends on the ratio of coalescence time, t_c, and contact time, $\bar{t}$ (Ross [29], Chesters [30]):

$$\lambda=\exp(-t_c/\bar{t}\ ). \tag{13}$$

The interaction time, $\bar{t}$, in most cases results from drop bouncing [30]. Assuming that the excess pressure in the film separating the drops results mainly from the deformation of the larger drop, Podgórska and Bałdyga [27, 28] derived the following relation:

$$\bar{t}=\frac{1}{2}\left[\frac{8}{3}\frac{R_S^3(\rho_D/\rho_C+\gamma)\rho_C}{\sigma(1+\zeta^3)}\right]^{1/2},\qquad \zeta=\frac{R_S}{R_L}. \tag{14}$$

The coalescence time, t_c, is a period of time necessary to decrease film thickness, h_f, from h_0 to the critical rupture thickness h_c. In the case of drops of low viscosity, μ_D, film drainage is controlled by the shear stresses exerted on the film by the liquid in the drop. Assuming a quasi-creeping flow created in the dispersed phase, the film drainage rate can be given as (Chesters [30]):

$$-\frac{dh_f}{dt}=\frac{2(2\pi\sigma/R_{eq})^{3/2}}{\pi\mu_D F^{1/2}}\ h_f^2, \tag{15}$$

where $R_{eq}=2R_SR_L/(R_S+R_L)$. The interaction force, F, can be estimated as $F=\pi a^2(2\sigma/R_L)$ (Podgórska and Bałdyga [27]) with the film radius, a, derived under the assumption that, in the case of drop bouncing, the whole kinetic energy is transformed into surface energy during film formation. For intermittent turbulence, the expression for coalescence time is given in the form, [27]:

$$t_c\cong 0.25\mu_D\ a\ \frac{R_{eq}^{3/2}}{\sigma R_L^{1/2}}\left[\frac{1}{h_c}\left(\frac{d_{jk}}{L}\right)^{0.016}-\frac{1}{h_0}\left(\frac{d_{jk}}{L}\right)^{-0.01}\right], \tag{16}$$

where $d_{jk}=(d_j+d_k)/2$.

3. The influence of large-scale inhomogeneity of turbulence on drop size

Large-scale inhomogeneity is related to highly inhomogeneous distributions of locally averaged properties of turbulence that influence the drop break-up and coalescence rates, such as the average rate of energy dissipation or the integral scale of turbulence. The time and space evolutions of drop size distribution can be predicted by solving the general population balance equation:

$$\frac{\partial n(\upsilon,\vec{x},t)}{\partial t}+\frac{\partial[u_i(\vec{x},t)n(\upsilon,\vec{x},t)]}{\partial x_i}=$$

$$= \frac{1}{2}\int_0^{\upsilon} h(\upsilon-\upsilon',\upsilon',\vec{x},t)\lambda(\upsilon-\upsilon',\upsilon',\vec{x},t)n(\upsilon-\upsilon',\vec{x},t)n(\upsilon',\vec{x},t)d\upsilon'$$

$$- g(\upsilon,\vec{x},t)n(\upsilon,\vec{x},t) - n(\upsilon,\vec{x},t)\int_0^{\infty} h(\upsilon,\upsilon',\vec{x},t)\lambda(\upsilon,\upsilon',\vec{x},t)n(\upsilon',\vec{x},t)d\upsilon'$$

$$+ \int_{\upsilon}^{\infty} \beta(\upsilon,\upsilon')\nu(\upsilon')g(\upsilon',\vec{x},t)n(\upsilon',\vec{x},t)d\upsilon'. \tag{17}$$

As direct linking of the complex coalescence and break-up kinetics proposed here (Equations (11)–(14) and (16)) to CFD is currently impossible, simpler models must be used. In our earlier works, we have considered the situation when the vessel content is divided into two cells, differing strongly in turbulence properties. For the case of pure drop break-up, we have considered two ideally mixed cells [24]. The local values of the rate of energy dissipation in the impeller zone $\langle\varepsilon_i\rangle$ and in the bulk $\langle\varepsilon_b\rangle$ and volume fractions of these regions, x_i and x_b, were calculated using the correlation of Okamoto, Nishikawa and Hashimoto [31]. This correlation was based on the experimental data of Sato, Kamiwano and Yamamoto [32], measured for a baffle tank with a Rushton turbine for a wide range of the impeller diameter to tank diameter ratio, $0.25 \leq D/T \leq 0.7$. The correlation was thus convenient for studying the influence of the impeller to tank diameter ratio on drop size. The difference of energy dissipation rates in the impeller zone and the bulk is so large that practically all the values of upper limit of integral α_x in Equation (11) in the bulk are smaller than $\alpha_{\min} = 0.12$, and one can assume that breakage occurs only in the impeller zone. When both break-up and coalescence take place, Podgórska and Bałdyga [27, 28] proposed a one-dimensional, single-circulation-loop, plug-flow model, which assumes that there are zones along the loop differing in turbulence properties. The loop was divided into cells characterized by local values of the average energy dissipation rate calculated using the correlation of Okamoto, Nishikawa and Hashimoto [31]. In the present paper, a multiple-cell model with ideally mixed cells is used, and the average properties of turbulence are calculated using CFD. A multiple-cell model was earlier used by Bourne and Yu [33], who investigated the influence of micromixing on product distribution for parallel reactions, and by Alopaeus, Koskinen and Keskinen [7], for liquid-liquid dispersions, but turbulence properties (energy dissipation rates) were based on measurements. To obtain the flow field and energy distribution in a Rushton tank, Bourne and Yu [33] used the data of Sato, Kamiwano and Hashimoto [32]. They divided the tank volume into 10 zones and obtained correlations for $\phi_j = \langle\varepsilon_j\rangle/\overline{\overline{\langle\varepsilon\rangle}}$ in these zones. According to their results, in the case of an impeller of the diameter ratio $D/T = 1/3$, 25% of the input energy is dissipated in the impeller swept volume, 45% – in the impeller stream volume, and 30% – in the bulk. According to Okamoto *et al.* [31], 74.3% of the input energy is dissipated in the impeller region, and this region is smaller than impeller swept and the impeller stream volumes in the 10-cell model of Bourne and Yu [33]. In this paper, we have used FLUENT 6.0 to model the hydrodynamics of a stirred tank equipped with a Rushton turbine and four baffles. A fine grid with 500 000 cells was

used. The grid was generated using the NetMeshGen and GAMBIT software. Two turbulence models were used: the standard k-ε model and the Reynolds stress model (RSM). To describe the motion of the Rushton turbine, a multiple reference model was applied. There was no free surface, and no slip condition was applied for any of the solid boundaries. Standard wall functions were assumed. Indeed, the predicted distribution of the rate of energy dissipation in the tank has a very nonuniform character (see Figure 4).

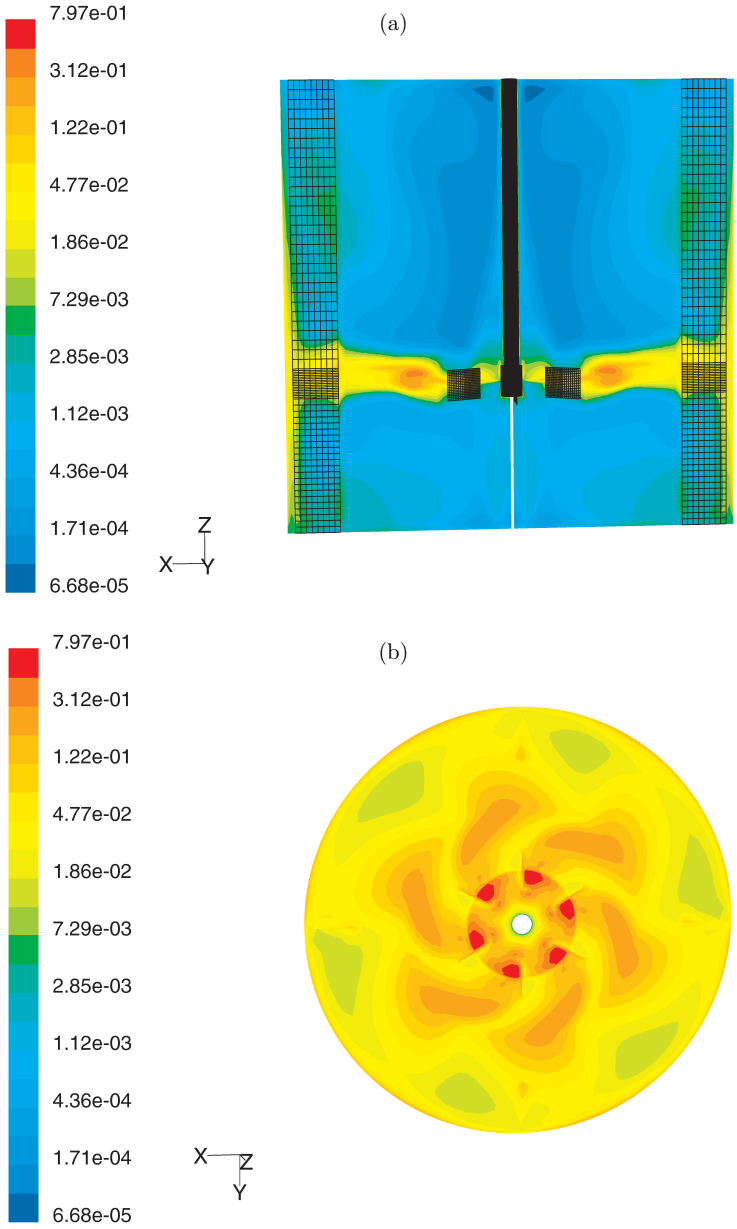

Figure 4. Contours of the energy dissipation rate in the tank ($T/D = 3$, $T = 0.24$m) predicted by RSM: (a) in the baffle plane, (b) in the Rushton turbine disk plane

Distributions of the normalized local turbulence energy dissipation rate in the region of the impeller stream for the baffle plane predicted by both models are shown in Figure 5. Both models predict double peaks. The RSM model predicts that energy dissipation rate for $r/R = 1.325$ is much higher than for smaller and greater radial distances, while the k-ε model predicts a decrease in the energy dissipation rate with the increase of the distance from the impeller blade.

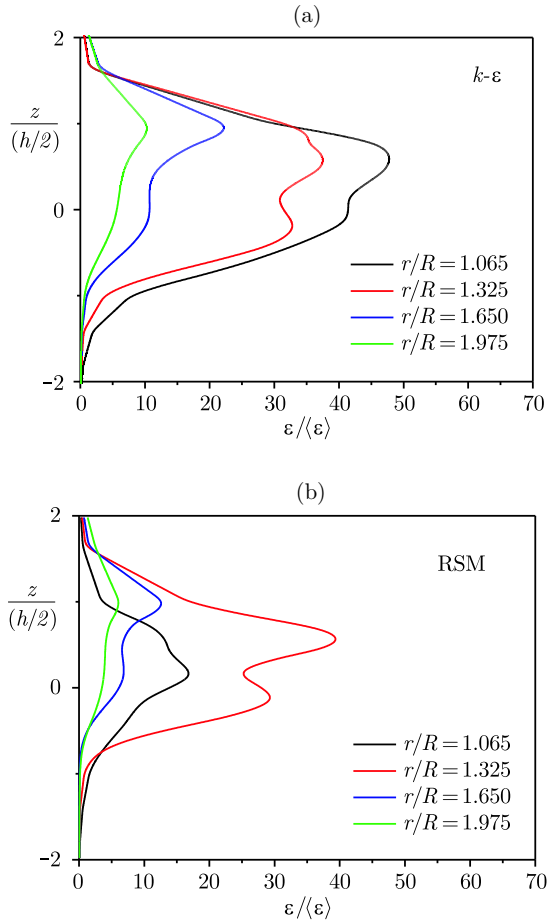

Figure 5. Normalized local energy dissipation rate in the impeller stream ($\theta = 0^{\circ}$): (a) k-ε model; (b) Reynolds stress model

For further calculations, the tank volume was divided into 10 cells similar to those of Bourne and Yu [33] (see Figure 6, where 1 – the impeller swept volume, 2 – the impeller stream volume, 3u and 3l – axial flow along a wall, 4u and 4l – flow near the top and bottom of the tank, 5u – flow along the shaft, 5l – flow under the impeller, 6u and 6l – flow between $r = R$ and $r = 0.4T$).

Both the k-ε and the RSM models predict a similar average dissipation rate in the impeller stream (2): $\phi_2 = 5.65$ according to the k-ε model, and $\phi_2 = 5.76$ according to the Reynolds stress model, which means that in this zone 46.87% (k-ε model) or 47.75% (RSM) of the total energy is dissipated, which agrees well with

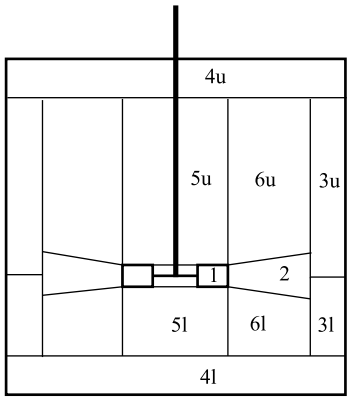

Figure 6. Zones chosen for simulation in a stirred tank

values given by Bourne and Yu [33]. In the impeller swept volume, the k-ε model predicts $\phi_1 = 22.46$ (16.7%) and RSM predicts $\phi_1 = 6.5$ (4.8%). Both models predict that the smallest energy dissipation rate is in the region 4u: $\phi_{4u} = 0.06$ (k-ε model) and $\phi_{4u} = 0.09$ (RSM). Normalized volume flow rates between cells, $Q_{ij} = K_{ij} N D^3/V$, have been calculated from mass flows through zone boundaries. The pumping capacity predicted by both models is similar: the k-ε model gives $K_{12} = 0.725$, and RSM gives $K_{12} = 0.715$. Calculations show that there is also flow from 3u to 6u, from 3l to 6l, from 6u to 5u and from 6l to 5l, not considered by Bourne and Yu [33]. Drop break-up and coalescence rates depend not only on the energy dissipation rate, but also on the scale of large eddies, L, so one also needs the distribution of average integral scale of turbulence in the tank. The local values of the scale of large eddies in all zones have been estimated as $L = (2k/3)^{3/2}/\varepsilon$. The smallest large eddies predicted by both models are in zone 1, and their size is $0.055D$ and $0.047D$, according to the k-ε and RS models, respectively. In the impeller stream zone we have $0.12D$ (k-ε) and $0.123D$ (RSM). The largest energetic eddies are in zones 5u and 6u – about $0.26D$ according to the k-ε model and $0.23D$ according to the RSM. Contours of scales of the large eddies predicted by the Reynolds stress model are shown in Figure 7.

Having specified energy dissipation rates and scales of large eddies in all zones, as well as flows between zones, population balance equations can be solved for each ideally mixed cell j:

$$\frac{\partial n_j(v,t)}{\partial t} = B_j - D_j + \sum_k Q_{kj} n_k(v,t) - n_j(v,t) \sum_j Q_{jk}. \tag{18}$$

4. Results and discussion

Calculations have been carried out for the following physical properties: $\mu_C = \mu_D = 0.001\,\mathrm{Pas}$, $\rho_C = \rho_D = 1000\,\mathrm{kg/m^3}$, $\sigma = 0.035\,\mathrm{N/m}$, with $A = 10^{-20}\,\mathrm{J}$. The Hamaker constant, A, affects critical film thickness, h_c, and the related coalescence time. Model constants for break-up, $C_g = 0.0035$, $C_x = 0.23$ have been determined by Bałdyga and Podgórska [24]. These constants were obtained by fitting to the experimental data of Konno, Aoki and Saito [8], and were later used with success for other systems. In the case of coalescence, a constant $C = 0.5$ was used in the expression for coalescence efficiency, ($\lambda(d_i, d_j) = \exp(-Ct_c/\bar{t}\,)$). The calculations were made

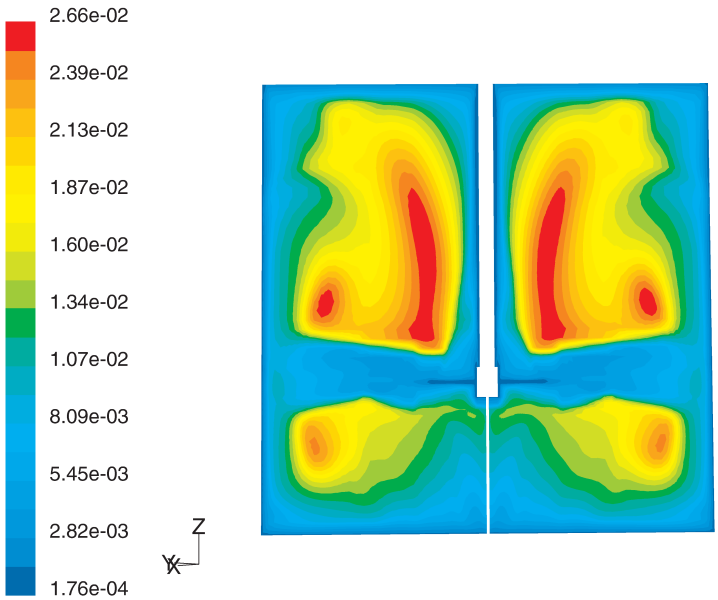

Figure 7. Contours of large-scale eddies' size $L(\theta = 45^{\circ})$

for Rushton tanks of $T/D = 3$ and $T/D = 2$, for which turbulence parameters were estimated for 10 vessel cells using CFD. In all the calculations, an experimentally determined power number, $P_0 = 5.5$, was used. Both turbulence models have predicted too low energy dissipation rate in the tank, but the normalized energy dissipation rates predicted by the k-ε model agree quite well with measurements [31–33]. The Reynolds stress model predicts much too small values of the energy dissipation rate in the impeller swept zone (1), so the k-ε model results have been used in further calculations. Figure 8 shows that neglecting large-scale inhomogeneity in a stirred tank results in considerable underestimation of the drop break-up rate. In fact, drop break-up takes place mainly in the impeller swept (1) and the impeller stream (2) zones, and the assumption of homogeneous energy dissipation in the tank leads to large errors.

Figure 9 shows the results of calculations for diluted dispersion, where coalescence was neglected. The drop size still changes after long agitation times, when rare, but most vigorous turbulent eddies play an important role.

Figure 10 shows that in a larger but geometrically similar tank, smaller drops are produced at the same average energy dissipation rate. This is connected with the fact that, in large system, integral scales of turbulence, L, affecting drop break-up (see Equation (11)) are greater. This scale-up effect results from the fact that, in a large scale system, the energetic cascade of eddies starts from more violent eddies of larger scale.

Figure 11 shows a comparison of break-up effects predicted with two multifractal models at long agitation times. The drop sizes from the She and Leveque [25] model (Equation (7)) are slightly larger than the sizes predicted with the spectrum measured by Meneveau and Sreenivasan [16]. This results from different values of $\alpha_{\min}$ in both models.

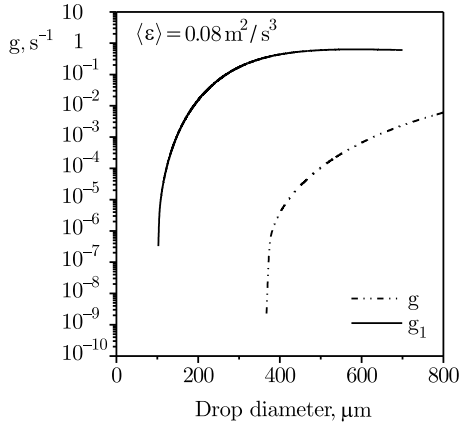

Figure 8. Comparison of the drop break-up rate in the impeller swept zone, g_1, and the drop break-up rate calculated under the assumption of homogeneous energy dissipation rate distribution in the tank, g

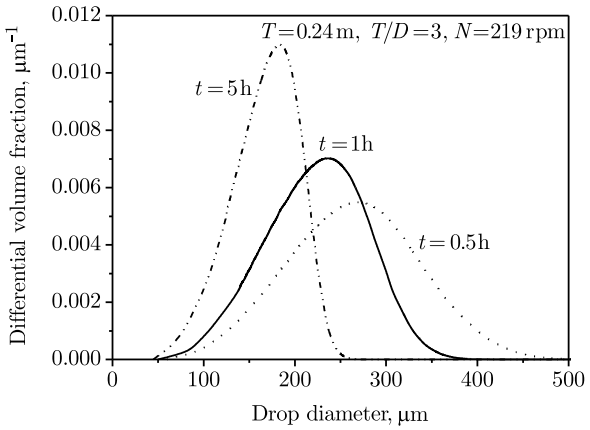

Figure 9. Transient drop size distribution for diluted dispersion

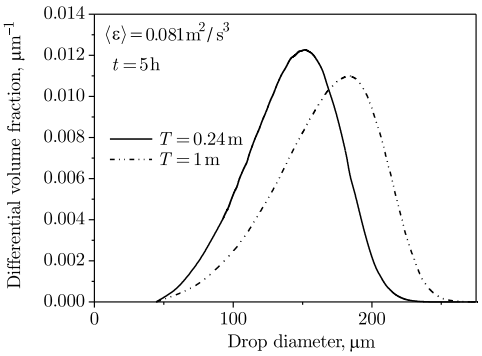

Figure 10. Effect of scale-up on drop size

Figure 12 illustrates the effect of model reduction from multi-cell to homogeneous distribution of turbulence properties. The difference in transient drop size distributions predicted by both models is significant.

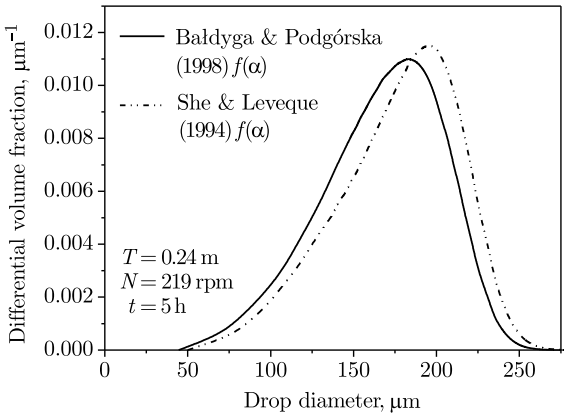

Figure 11. Comparison of drop size distributions predicted by various multifractal models

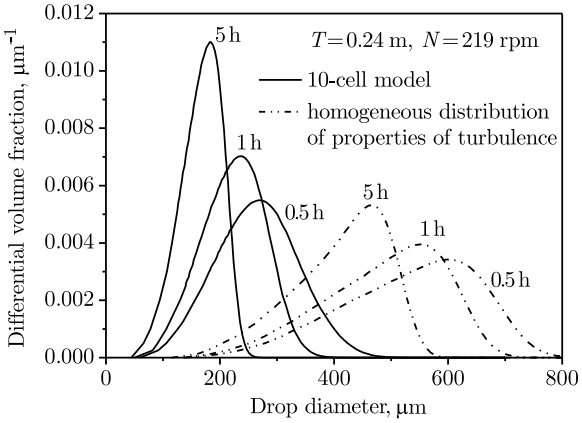

Figure 12. Transient drop size distributions predicted by the multiple-cell model and the model based on homogeneous distribution of properties of turbulence in the tank

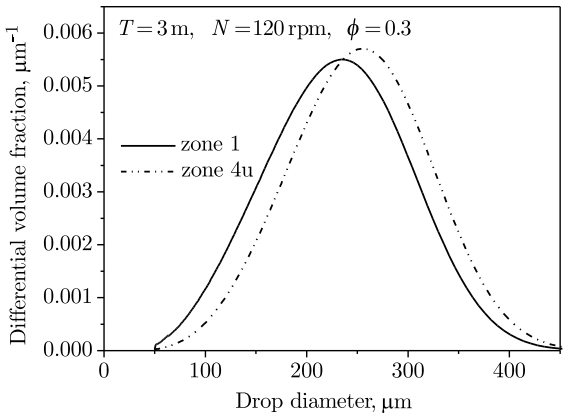

Figure 13. Spatial distribution of drop size in a coalescing system

Figures 13 shows a small variation of drop size with the position in the tank in breaking-up and coalescing dispersion. This effect is observed only for large scale systems with long circulation times.

Figure 14 is a comparison of the 10-cell model predictions with the experimental data of Konno, Muto and Saito [34] for highly coalescing dispersion. Good agreement of measured and calculated drop size distributions is observed for short and long agitation times.

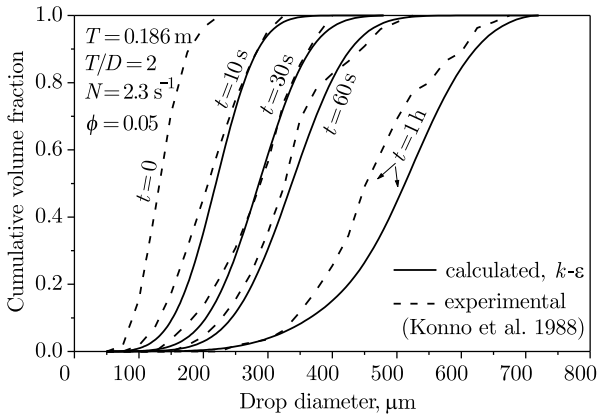

Figure 14. Comparison of model predictions with experimental data

The presented results show that both types of inhomogeneity of turbulence in a stirred tank, *i.e.* small-scale and large-scale, should be taken into account to explain some of the effects observed experimentally which cannot be explained with the classic theory of turbulence and to successfully predict drop size distribution.

Acknowledgements

This work was supported by the special program *Dynamics of Complex Systems* of the Warsaw University of Technology.

References

[1] Kolmogorov A N 1949 *Doklady Akademii Nauk SSSR* **66** 825 (in Russian)
[2] Hinze J O 1955 *AIChE Journal* **1** 289
[3] Kolmogorov A N 1941 *Doklady Akademii Nauk SSSR* **30** 299 (in Russian)
[4] Coulaloglou C A and Tavlarides L L 1977 *Chem. Engng. Sci.* **32** 1289
[5] Tsouris C and Tavlarides L L 1994 *AIChE Journal* **40** 395
[6] Svendsen H F and Luo H 1996 *Canadian J. Chem. Engng.* **74** 321
[7] Alopaeus V, Koskinen J and Keskinen K J 1999 *Chem. Engng. Sci.* **54** 5887
[8] Konno M, Aoki M and Saito S 1983 *J. Chem. Engng. Japan* **16** 312
[9] Kuriyama M, Ono M, Tokanai H and Konno H 1996 *Trans. Inst. Chem. Engng.* **A 74** 431
[10] Lam A, Sathyagal AN, Kumar S and Ramkrishna D 1996 *AIChE Journal* **42** 1547
[11] Konno M and Saito S 1987 *J. Chem. Engng. Japan* **20** 533
[12] Bałdyga J and Bourne J R 1995 *Chem. Engng. Sci.* **50** 381
[13] Bałdyga J, Podgórska W, Zawada D and Żuławnik D 1998 *Proc. XVI Polish Conf. Chemical and Process Engineering*, Cracow, Poland, vol. **4**, pp. 8–11
[14] Bałdyga J, Bourne J R, Pacek A W, Amanullah A and Nienow A W 2001 *Chem. Engng. Sci.* **56** 3377
[15] Pacek A W, Chamsart S, Nienow A W and Bakker A 1999 *Chem. Engng. Sci.* **54** 4211
[16] Meneveau C and Sreenivasan K R 1991 *J. Fluid Mech.* **224** 429
[17] Batchelor G K and Townsend A A 1949 *Proc. R. Soc.* **A 199** 238
[18] Frisch U, Sulem P L and Nelkin M 1978 *J. Fluid Mech.* **87** 719

[19] Frisch U and Parisi G 1985 *Turbulence and predictability in geophysical fluid dynamics and climate dynamics* (Ghil M, Benzi R and Parisi G, Eds.), Amsterdam, North-Holland, pp. 84–88
[20] Chhabra A and Jensen R 1989 *Phys. Rev. Lett.* **62** 1327
[21] Meneveau C and Sreenivasan K R 1987 *Nuclear Phys.* **B 2** 49
[22] Kolmogorov A N 1962 *J. Fluid Mech.* **13** 82
[23] Obukhov A M 1962 *J. Fluid Mech.* **13** 77
[24] Bałdyga J and Podgórska W 1998 *Canadian J. Chem. Engng.* **76** 456
[25] She Z S and Leveque E 1994 *Phys. Rev. Lett.* **72** 336
[26] Bałdyga J and Bourne J R 1993 *J. Chem. Engng. Japan* **26** 738
[27] Podgórska W and Bałdyga J 2000 *Proc. 10th European Conf. Mixing*, Delft, The Netherlands, Amsterdam, Elsevier, pp. 141–148
[28] Podgórska W and Bałdyga J 2001 *Chem. Engng. Sci.* **56** 741
[29] Ross S L 1971 *Measurements and Models of the Dispersed Phase Mixing Process*, PhD Thesis, University of Michigan, Ann Arbor
[30] Chesters A K 1991 *Trans. Inst. Chem. Engng.* **A 69** 259
[31] Okamoto Y, Nishikawa M and Hashimoto K 1981 *Int. Chem. Engng.* **21** 88
[32] Sato Y, Kamiwano M and Yamamoto K 1970 *Kagaku Kogaku* **34** 104
[33] Bourne J R and Yu S 1994 *Ind. Engng. Chem. Res.* **33** 41
[34] Konno M, Muto T and Saito S 1988 *J. Chem. Engng. Japan* **21** 335